ARTICLE NO. 79-0072R

Direct Testing of Subgrid-Scale Models

O. J. McMillan*
Nielsen Engineering & Research, Inc., Mountain View, Calif.
and
J. H. Ferziger†
Stanford University, Stanford, Calif.

Results are given from a study in which models used in large-eddy simulation of turbulent flow are tested using results of exact simulations of the Navier-Stokes equations. The results to date are for models of the eddy-viscosity type applied to incompressible homogeneous turbulence (either isotropic or in the presence of applied irrotational plane strain). The comparisons are by means of correlation coefficients; model parameters are calculated by matching the rms magnitudes of the exact and modeled quantities. Effects on these correlation coefficients and model parameters are shown for variations in attributes of the large eddy simulation (e.g., filter type and width and differencing method) as well as in parameters of the flow simulated (e.g., Reynolds number and strain rate).

Nomenclature

a = mean strain rate in x_1 direction
b = mean strain rate in x_2 direction
C = correlation coefficient, Eq. (4)
C_c = parameter in constant-eddy-viscosity model
C_q = parameter in subgrid-scale kinetic-energy model
C_s = parameter in Smagorinsky model
C_v = parameter in vorticity model
c = mean strain rate in x_3 direction
G = spatial filter function, see Appendix
M = modeled quantity in Eq. (4)
M_{ij} = subgrid-scale stress model
N = time step in Navier-Stokes solution, time = $0.0073N$ seconds
R_{sgs} = subgrid-scale Reynolds number, $\bar{S}\Delta_a^2/\nu$
R_λ = Reynolds number based on Taylor microscale
$\bar{S}$ = rms strain rate of filtered field
$\hat{S}_{ij}$ = rate-of-strain tensor for filtered field, $\frac{1}{2}(\partial\tilde{u}_i/\partial x_j + \partial\tilde{u}_j/\partial x_i)$, or rate-of-strain tensor for the mean and filtered fields, Eq. (6)
t = time
t_d = dissipation time scale, Eq. (7)
t_s = strain time scale, Γ^{-1}
U_i = mean velocity component in ith direction, flow with mean strain, Eq. (5)
u_i = instantaneous velocity component in ith direction
$\tilde{u}_i$ = filtered velocity component in ith direction, Eq. (1)
u_i' = subgrid-scale velocity component in ith direction, $u_i - \tilde{u}_i$
X = exact quantity in Eq. (4)
x_i = spatial coordinate
Γ = mean strain rate
γ = constant in Gaussian filter, Eq. (A2)
Δ = grid spacing for 64^3 grid
Δ_a = length scale for filter function, isotropic filter
Δ_{ai} = length scale in ith direction for filter function, anisotropic filter
Δ_b = length scale for box filter, Fig. 7
Δ_c = grid spacing for coarse grid
ϵ = viscous dissipation rate of turbulence kinetic energy per unit mass
ν = kinematic viscosity
ν_T = eddy viscosity
τ_{ij} = subgrid-scale stress, Eq. (2)
ω_i = instantaneous vorticity component in ith direction

Subscripts

$1,2,3;i,j,k$ = coordinate directions

Superscripts

$\bar{(\ )}$ = filtered variable
$(\ )'$ = subgrid-scale variable

I. Introduction

TURBULENCE modeling has made considerable strides in the past two decades and is driven largely by the need for better means of predicting flows in a variety of devices. The testing of these models has, until recently, been a highly empirical affair. It is nearly impossible to measure experimentally all of the factors needed to test models, so it has often been necessary to rely on indirect methods of comparing calculations done using the models with the phenomena they are supposed to represent.

It is possible to use computed flows as the basis for testing models. The difficulty here is that only a few simple turbulent flows can be computed with sufficient accuracy. While this approach could be implemented in several ways, the one which provides the most information of the best accuracy uses exact Navier-Stokes simulations to test the subgrid-scale models required in large-eddy simulation. Large-eddy simulation is a method midway between exact simulation and time-averaged modeled computation, which computes the large eddies explicitly and models only the small ones. The terms to be modeled are analogous to those in the time-averaged equations and the same models should be valid in either case. Therefore, conclusions about time-averaged

Presented as Paper 79-0072 at the AIAA 17th Aerospace Sciences Meeting, New Orleans, La., Jan. 15-17, 1979; submitted Feb. 2, 1979.

Index categories: Computational Methods; Viscous Nonboundary-Layer Flows.

*Research Engineer. Member AIAA.
†Professor, Mechanical Engineering Department; also, Consultant, Nielsen Engineering & Research, Inc. Member AIAA.

models can be drawn by inference from the results of using exact simulations to test subgrid-scale models.

The method we use is derived from that of Clark[1] and is outlined in Sec. II. We have used this method to look at the effects of the filter characteristics (type and width), the numerical method used in the large-eddy simulation, and important parameters such as the Reynolds number and strain rate. The results of these calculations are presented and discussed in Sec. III, and the final section contains the conclusions from this work. Further details can be found in Refs. 2 and 3.

II. Methodology

In this paper, we use the results from direct simulations of the Navier-Stokes equations to test subgrid-scale models of the eddy-viscosity type. The direct simulations were done by R. S. Rogallo[4] on the ILLIAC IV at the NASA Ames Research Center. He calculates the evolution of incompressible homogeneous turbulence with or without simple strain. The 64^3 grid used allows simulation of flows with Taylor-microscale Reynolds number R_λ up to about 40. The results, which can be considered to be exact, are furnished on a magnetic tape containing the velocity field at an instant in time.

Imagine that the same flow is to be calculated by means of large-eddy simulation on a coarser (16^3) grid. In this approach, one attempts to calculate the behavior of the large-scale componets of turbulence, while the small scales are modeled; a review is given in Ref. 5. The large-scale velocity field $\bar{u}_i$ is obtained by filtering the velocity field

$$\bar{u}_i = \int G(x-x')\,u_i(x')\,dx' \tag{1}$$

Here, G is an appropriate filter function, the intergration is over the entire flowfield, and u_i' is the subgrid-scale field defined by $u_i' = u_i - \bar{u}_i$. The filter functions used in this work are presented in the Appendix. The filtered Navier-Stokes equations contain terms $\overline{u_i'u_j'}$ which play the role of subgrid-scale Reynolds stresses; these are the terms which are to be modeled. Because we know the exact value of u_i at each point on the 64^3 grid, we can calculate the exact values of $\bar{u}_i$, u_i', and the subgrid-scale stress on the 64^3 grid, and extract the appropriate values on the coarse (16^3) grid. On this 16^3 grid, we can also calculate what eddy-viscosity models would predict for the subgrid-scale stress, since these models represent this quantity as a functional of the $\bar{u}_i$ field. Note that this is what a model would produce if it were applied to the *exact* resolvable field; in an actual large-eddy simulation, it is applied to a resolvable field computed with the use of the model, which is somewhat different.

We can use the exact and "modeled" values for the subgrid-scale stress to assess the accuracy of the models. In the remainder of this section, we define some terms and present the models used. For a more detailed description see Ref. 2.

The subgrid-scale stress is defined to be

$$\tau_{ij} = \tfrac{1}{3}\delta_{ij}\overline{u_k'u_k'} - \overline{u_i'u_j'} \tag{2}$$

In eddy-viscosity models, the subgrid-scale stress is represented as proportional to the rate of strain of the resolvable-scale field

$$\tau_{ij} = 2\nu_T\bar{S}_{ij} = \nu_T\left(\frac{\partial\bar{u}_i}{\partial x_j} + \frac{\partial\bar{u}_j}{\partial x_i}\right) \tag{3}$$

The models for ν_T evaluated are:

1) The Smagorinsky model, $\nu_T = (C_s\Delta_a)^2\,[2\bar{S}_{ij}\bar{S}_{ij}]^{1/2}$, where Δ_a is the filter length scale and C_s is the model parameter.

2) The vorticity model, $\nu_T = (C_v\Delta_a)^2(\bar{\omega}_i\bar{\omega}_i)^{1/2}$, where $\bar{\omega}_i = \epsilon_{ijk}\partial\bar{u}_k/\partial x_j$.

3) The kinetic energy model, $\nu_T = (C_q\Delta_a)\,(\tfrac{1}{3}u_k'u_k')^{1/2}$.

4) The constant-eddy-viscosity model, $\nu_T = C_c$.

The assessment of the accuracy of a modeled quantity M in representing an exact quantity X is done in terms of a correlation coefficient

$$C(M,X) = \langle MX\rangle/\langle M^2\rangle^{1/2}\langle X^2\rangle^{1/2} \tag{4}$$

where $\langle\ \rangle$ represents an average over the 16^3 grid. The magnitude $|C(M,X)|$ will vary between 0 (if M and X are totally unrelated) to 1 (if the model is exact to within a multiplicative constant). It is independent of the value used for the parameter in a given model. Values of the parameters can be determined, however, by forcing agreement of the root mean square (rms) modeled and exact values. Statistics would suggest that this is not the best choice for the parameter, but we have found that this choice produces the best results. For further discussion see Ref. 3.

The results can be calculated on the three levels used by Clark[1]: 1) the tensor level, where models M_{ij} are compared directly to the exact subgrid-scale stress τ_{ij}; 2) the vector level, where $\partial M_{ij}/\partial x_j$ is compared to $\partial\tau_{ij}/\partial x_j$; and 3) the scalar level, where $\bar{u}_i\,\partial M_{ij}/\partial x_j$ is compared to $\bar{u}_i\,\partial\tau_{ij}/\partial x_j$. At the tensor and vector levels, we will present the average of the coefficients for the various components.

All differentiation on the 64^3 grid (e.g., to calculate the exact value of $\partial\tau_{ij}/\partial x_j$) is done using Fourier or pseudospectral differencing. The differentiation required in the model calculations on the 16^3 grid is done using any of three methods: second-order central differencing, fourth-order central differencing, or pseudospectral differencing.

III. Results and Discussion

Clark[1] evaluated the eddy-viscosity models treated here for one homogeneous isotropic flowfield and one choice of filter. Our first task was to reproduce the calculations done by Clark. Following that, we have done various extensions of Clark's work.

A. Comparison with the Results of Clark

Our calculations are totally independent of Clark's. He did his own direct simulation and had his own data reduction routine. For this comparison, we did the calculations with the same ("box") filter and filter width as Clark. Table 1 summarizes the parameters and methods used in both in-

Table 1 Summary of parameters and methods of present work and those of Clark[1]

	Clark	Present work
Navier-Stokes solution	Ref. 1	Ref. 4
Grid (spacing = Δ)	64^3	64^3
Space differencing	Fourth-order finite difference	Spectral
Time differencing	Third-order predictor-corrector	Fourth-order Runge-Kutta
Initial energy spectrum	From Ref. 6	Same as Clark's
$(R_\lambda)_{\text{initial}}$	38.1	Same as Clark's
Filtered fields		
Grid	8^3	16^3
Filter	Box	Box
Filtering length scale, (Δ_a)	8Δ	8Δ
Model derivatives	Fourth-order finite difference	Variable (see text)

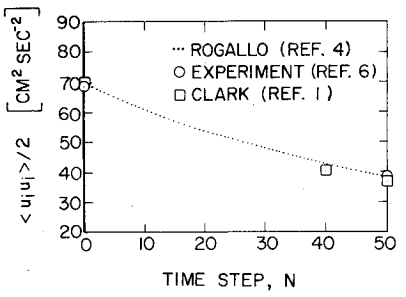

Fig. 1 Turbulence kinetic energy per unit mass as a function of time step; note shifted origin.

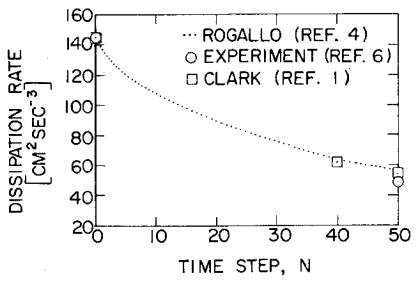

Fig. 2 Viscous dissipation rate per unit mass as a function of time step; note shifted origin.

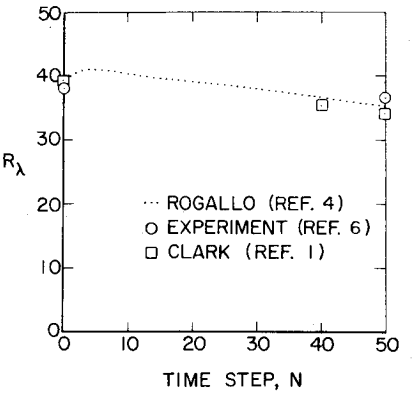

Fig. 3 Taylor-microscale Reynolds number as a function of time step.

vestigations. There are differences in the "exact" velocity fields produced; however, from Figs. 1-3, we see that the time dependence of the kinetic energy, dissipation rate, and Taylor-microscale Reynolds number found by Rogallo agrees with both Clark's and experimental values.[6] Clark chose the velocity field at time step 40 for detailed analysis, and we have done the same.

The differences between our work and Clark's are as follows. We used a 16^3 coarse grid because it gives improved statistics relative to the 8^3 grid used by Clark; this is expected to be a small effect. We used three differencing methods on our coarse grid whereas Clark used a fourth-order method on his coarse grid. The effect on our results of changing the differencing method used is discussed in detail in a later section. In this section, we compare Clark's results to ours calculated using both second-order and fourth-order central differencing; the truncation error for Clark's differencing method is bounded by the truncation errors for these methods.

In Table 2, the correlation coefficients and model parameters calculated in the present work and by Clark are shown. Examination shows that the differences between the calculations are slight. The greatest difference is the lack (in the present work) of an increase in the correlation coefficients in going from the tensor to the vector level. This and the small differences in the parameters are felt to be due to small differences in the velocity fields and the different coarse grids used. In any case, the differences are not large enough to modify Clark's conclusions; the major one is that all of the models investigated essentially perform equally well. A model using the exact kinetic energy in the subgrid-scale field is only a slight improvement on the algebraic models. Because of this conclusion, the results presented in the remainder of this paper will be for the Smagorinsky model only. The results shown for it are representative of those derived for the other models.

B. Filter Type

In previous work on large-eddy simulation[7] the choice of filter type was found to have only minor effects on the results of simulation. We have investigated the Gaussian and "box" filters using our direct testing methods and the previously mentioned flowfield. The same filter width ($\Delta_a = 2\Delta_c$) was used for both filters. The results verify that the choice of filter type is a matter of the user's preference. Accordingly, the results presented in the remainder of this paper were obtained using a Gaussian filter.

C. Filter Width

A more significant parameter is the filter width. The filter must be wide enough to eliminate any structures that are smaller than the computational grid. On the other hand, if the width is too large, most of the interesting structure will be

Table 2 Comparison of present results to those of Clark (Ref. 1)

	Average correlation coefficient			Model parameter		
	Present work			Present work		
Tensor level	Second order	Fourth order	Ref. 1	Second order	Fourth order	Ref. 1
Smagorinsky	0.33	0.32	0.28	0.20	0.17	0.25
Vorticity	0.32	0.32	0.26	0.22	0.19	0.28
Kinetic energy	0.36	0.35	0.30	0.16	0.14	0.18
Constant ν_T	0.35	0.34	0.30	—	—	—
Vector level						
Smagorinsky	0.29	0.28	0.35	0.23	0.18	0.26
Vorticity	0.30	0.29	0.33	0.25	0.20	0.25
Kinetic energy	0.32	0.31	0.36	0.21	0.15	0.16
Constant ν_T	0.31	0.30	0.36	—	—	—
Scalar level						
Smagorinsky	0.54	0.53	0.58	0.17	0.14	0.17
Vorticity	0.55	0.55	0.58	0.19	0.15	0.19
Kinetic energy	0.58	0.57	0.61	0.12	0.09	0.10
Constant ν_T	0.56	0.56	0.61	—	—	—

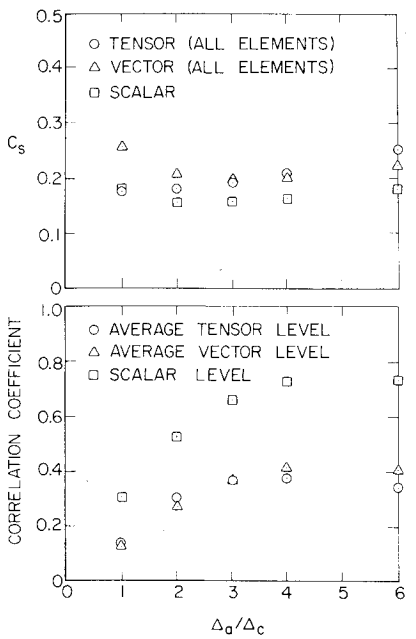

Fig. 4 Correlation coefficients and model parameters as a function of filter width, Smagorinsky model, $R_\lambda = 37$, Gaussian filter.

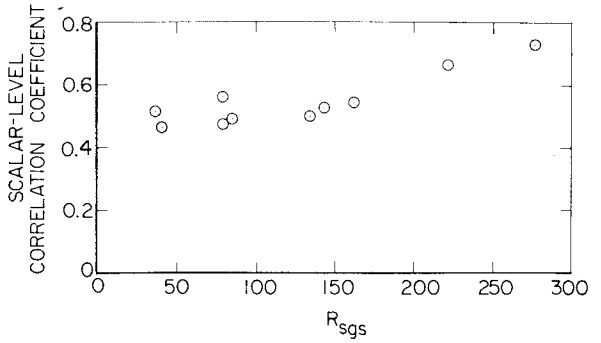

Fig. 5 Scalar-level correlation coefficient as a function of subgrid-scale Reynolds number for the Smagorinsky model.

eliminated and a large part of the computation will be wasted. Therefore, there is an optimum filter width. Using the same flowfield as previously, and using second-order central differences in the model calculations, we have investigated a Gaussian filter of varying width. Figure 4 shows the correlation coefficients and model parameters obtained as a function of filter width for the Smagorinsky model. The correlation increases with increasing width of the filter, but the rate of increase decreases. The model parameter (C_s) is large at small filter widths and decreases as the width is increased; there is a plateau and at higher values of the width, the parameter increases again.

The fraction of viscous dissipation occurring in the subgrid scales increases with Δ_a/Δ_c; the derivations of the models require that the dissipation be in the subgrid scales, so the increased correlation is not surprising. However, as the filter width becomes large, very little of the energy in the actual flow is captured in the resolvable scales—an obviously undesirable situation. Taking all of these factors into account (staying in the "plateau" region of the model parameter, maximizing the model correlation coefficient while regaining a reasonable portion of the energy in the resolvable field), the best filter width to use is between two and four times the width of the mesh on which the large-eddy simulation is to be conducted. This range corresponds, for the flows considered here, to requiring that at least 80% of the actual dissipation occur in the subgrid-scale field and at least 10% of the total energy remain in the resolved field. These should be useful guidelines for those doing large-eddy simulations, but they should, of course, be checked in other flows.

D. Finite-Difference Method

In an examination of the effect of the choice of differencing method on the results of large-eddy simulation,[8] it was found that the model parameter that matches the experimental energy decay rate in homogeneous isotropic turbulence is essentially independent of the differencing scheme used.

We calculated the model correlation coefficients and parameters using fourth-order central differencing and pseudo-spectral differencing and compared them to the second-order central differencing results. The results are displayed in Table 3.

The correlation coefficient is nearly independent of the differencing method used, but the model parameter strongly depends on the differencing method. In spite of the results of Ref. 8, this is not unexpected, since the differencing methods should produce different strain rates. The difference between our result and Ref. 8 may be due to using a directly simulated flowfield to derive the parameter vs using a flowfield calculated using the model. At any rate, the results of Table 3 should be of interest as a guide to those doing large-eddy simulation.

E. Reynolds Number

We expect that the subgrid-scale turbulence (and the model used to approximate it) must depend on a Reynolds number. The natural length scale is the filter width Δ_a, which is also used in the models. The velocity scale is more difficult to determine, but we expect that it ought to be proportional to the rms strain rate $\bar{S}$ of the resolvable scale and the filter width. Therefore, we have used $\bar{S}\Delta_a^2/\nu = R_{sgs}$ as the representative Reynolds number of the subgrid scale. The importance of this is that in a wall-bounded flow, R_{sgs} will vary from a high value in the free flow to very low values near the wall. This is also a difficult problem theoretically.

The Reynolds number can be varied by changing any of the quantities contained in it. For a given realization of a flow, ν is fixed and, as the filter width Δ_a is increased, the strain rate goes down. When this is coupled to the limited range of Δ_a for which the models are meaningful (see above), we find that only a limited range of Reynolds number can be obtained from a single realization. For this reason, Rogallo furnished several flowfields with different values of R_λ (in the range 5-40). These variations also give different values of R_{sgs}, so in this way we were able to cover a fairly wide range of Reynolds number.

Table 3 Effect of differencing method on average correlation coefficients and parameters for the Smagorinsky model

	Correlation coefficient Differencing method			Model parameter Differencing method		
Level	Second order	Fourth order	Pseudo-spectral	Second order	Fourth order	Pseudo-spectral
Tensor	0.30	0.30	0.29	0.18	0.16	0.14
Vector	0.27	0.27	0.24	0.21	0.16	0.13
Scalar	0.53	0.52	0.50	0.16	0.12	0.10

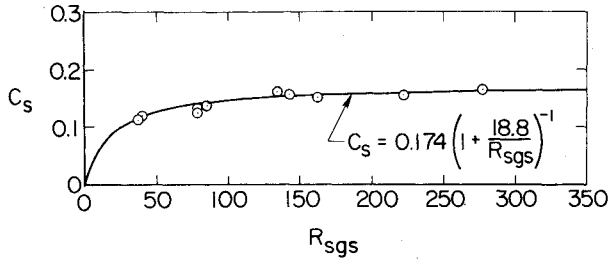

Fig. 6 Scalar-level model parameter as a function of subgrid-scale Reynolds number for the Smagorinsky model. Second-order central differencing used in the model calculations.

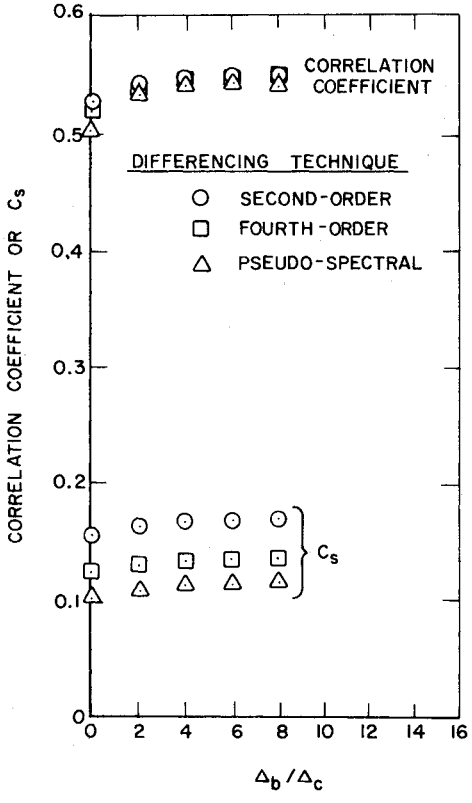

Fig. 7 Effect on scalar-level correlation coefficient and C_s of the modified Smagorinsky model of Ref. 13.

Figure 5 shows the dependence on R_{sgs} of the scalar-level correlation coefficients determined for the Smagorinsky model using the second-order, central-differencing method. The flowfields at several values of R_λ were analyzed with Gaussian filters of varying widths, subject to the constraints developed earlier—at least 80% of the viscous dissipation must be in the subgrid scales and at least 10% of the total energy must remain in the resolved field. From Fig. 5 it appears that the correlation ceofficient increases slightly with increasing Reynolds number. This is expected theoretically.

The dependence on R_{sgs} of the scalar-level model parameter is shown in Fig. 6. Comparable curves obtained for the other differencing methods are shown in Ref. 3. The parameter displays a definite Reynolds number dependence. Fortunately, it nearly reaches its high Reynolds number asymptote within the range covered. The value of the parameter that we find as the high R_{sgs} asymptote is within the range of values that have been used previously (0.1-0.24, Refs. 7 and 9-11) to fit experiments at Reynolds numbers above those that we were able to cover. Agreement with Lilly's theoretical high-R_λ value (0.22, Ref. 12) is fair. The computed values of Fig. 6 have been fit by an approximate expression for the Reynolds number dependence derived in Ref. 3.

F. Miscellaneous Investigations

In the work just described, each set of correlation coefficients and model parameters was derived from a single realization of the flow. To obtain different realizations, we asked Rogallo to vary the initial phases of the Fourier velocity components in his simulations. Two additional realizations of the homogeneous isotropic turbulent flow described in Figs. 1-3 were calculated and model correlation coefficients and parameters were calculated at time step 40 in each of these realizations using a Gaussian filter ($\Delta_a/\Delta_c = 2$). The effects were negligible.

Based on studies using Burger's equation and the direct interaction approximation, Love and Leslie[13] suggested modifying the Smagorinsky model by replacing the local value of $[2\bar{S}_{ij}\bar{S}_{ij}]^{1/2}$ by the square root of an average over a large volume. They obtained improved results using this nonlocal version, and recommended testing this approach on "Navier-Stokes turbulence." Such a test was carried out for one case. The extent of the volume over which $2\bar{S}_{ij}\bar{S}_{ij}$ was averaged was varied. The results for the three different differencing schemes are shown in Fig. 7. In this figure, Δ_b is the filter width of the "box" filter used to do the volume averaging. It is seen that the correlation is only slightly improved by the volume-averaging procedure, and that the effect on C_s is small.

The effect of filtering on the resolvable-scale, velocity-gradient skewness and flatness was examined. It was demonstrated that large-eddy simulation cannot be extrapolated reliably to zero filter width to obtain skewness or flatness, confirming a result found in Ref. 7.

G. Homogeneous Turbulence in the Presence of Mean Strain

Strain in the mean field is known to have an important effect on the structure of the turbulence. Presumably, mean strain should also affect the structure of the subgrid-scale turbulence, and should affect the modeling in some way. Since the mean strain occurs in the largest scales, we would expect that its effect would be the largest on the large scales. This might mean, for example, that in the model, the mean strain and the strain created by the resolvable field should be treated differently.

The code of Ref. 4 can compute the case of homogeneous turbulence acted on by irrotational mean strain. In this case, the velocity field is decomposed as

$$u_i = U_i + \tilde{u}_i + u_i' \tag{5}$$

where $U_1 = ax_i$, $U_2 = bx_2$, $U_3 = cx_3$ is the imposed field, and $\tilde{u}_i$ and u_i' are the resolvable and subgrid-scale velocity fields, respectively. The mean strain rates a, b, and c are functions of time only and $a+b+c=0$ as required by continuity. In the initial results presented in this section, the strain-rate tensor, which appears in the eddy viscosity models, is formulated as:

$$\tilde{S}_{ij} = \frac{1}{2}\left[\frac{\partial}{\partial x_j}(U_i+\tilde{u}_i) + \frac{\partial}{\partial x_i}(U_j+\tilde{u}_j)\right] \tag{6}$$

and we have treated the case of plane strain with constant strain rate, i.e., $a = -b = \Gamma$, $c = 0$.

In this flow, two important time scales are the dissipation time scale,

$$t_d = \langle (\tilde{u}_i + u_i')(\tilde{u}_i + u_i') \rangle / 2\epsilon \tag{7}$$

where ϵ is the dissipation rate per unit mass, and the strain time scale, $t_s = \Gamma^{-1}$.

We have investigated the effect of the ratio of these time scales on subgrid-scale modeling. Rogallo ran three cases with different strain rates (Γ), each with the initial energy spectrum used in the isotropic flows discussed earlier. The resulting values of t_s/t_d are shown in Fig. 8 as a function of strain ratio

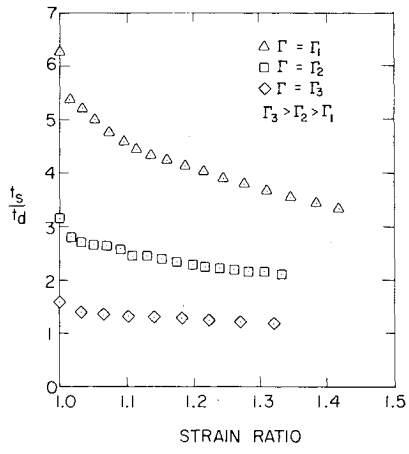

Fig. 8 Ratio of time scales as a function of strain ratio.

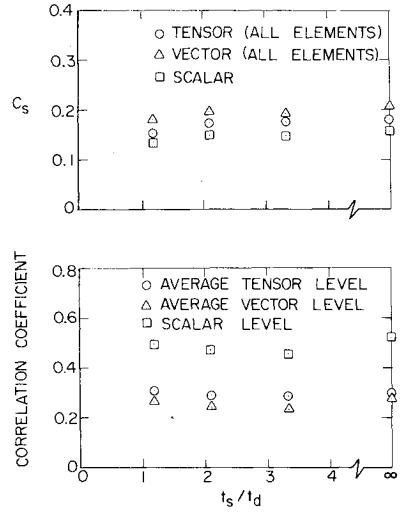

Fig. 9 Correlation coefficients and model parameters for the Smagorinsky model as a function of time-scale ratio.

$\exp(\Gamma t)$. Sudden distortion theory suggests this quantity is the controlling parameter.

The strain ratios achieved are in the vicinity of 1.3 to 1.4. This is a very modest amount of straining, but it is the most that can be accurately simulated using the code of Ref. 4 at present. We hope to investigate higher strain ratios in the future, but this depends on some modifications being made to the code. Higher strain rates will also be studied.

The Smagorinsky model correlation coefficients and model parameters calculated for the three terminal flowfields are shown in Fig. 9. In these calculations, second-order central differencing and an isotropic Gaussian filter with $\Delta_a/\Delta_c = 2$ were used. The limiting values for isotropic turbulence ($t_s/t_d \to \infty$) are shown for comparison. This figure shows that for the range of strains and time-scale ratios covered, there is no significant effect on the subgrid-scale model.

H. Definition of $\bar{S}_{ij}$ in Model Calculations

It might be necessary for a subgrid-scale model to differentiate between the mean strain and the resolvable-scale strain. We examined the effects on the subgrid-scale models of using only the resolvable turbulence strain rate where a strain-rate tensor is required in the models. For the highest mean strain rate treated thus far, however, the rms resolvable-scale strain rate is only 12% less than that calculated using Eq. (6), so only small effects should be discernible. We calculated the correlation coefficients and model parameters resulting from both definitions of $\bar{S}_{ij}$ and, as expected, the differences were small. However, the differences increased as t_s/t_d decreased, so this question should be reinvestigated when larger mean strain rates are studied.

I. Anisotropic Filters

A final investigation was made using one of these strained flowfields. In wall-bounded flows, it is necessary to use highly distorted meshes near the boundaries. In these cases, anisotropic filters are desirable and the appropriate length scale in the subgrid-scale model is no longer obvious. Two possible choices of length scale are $(\Delta_{a_1}\Delta_{a_2}\Delta_{a_3})^{1/3}$ and $(\Delta_{a_i}\Delta_{a_j})^{1/2}$. Which of these is most appropriate can be assessed by examining the tensor-level model parameters associated with each for a given choice of anisotropic filter—the one exhibiting the least variability is obviously the best choice. We have looked at this question using the flowfield with $t_s/t_d = 1.18$ and the anisotropic filter described below (Eq. (6) was used to define $\bar{S}_{ij}$). Because the mean strain ratio in each coordinate direction is known for this flowfield, we can choose the filtering length scales such that they remain a constant multiple of the length of the sides of a strained fluid element. That is,

$$\Delta_{a_1}/\Delta_c = 2\exp\left(\int_0^t a\,d\tau\right) = 2\exp(\Gamma t) \tag{8a}$$

$$\Delta_{a_2}/\Delta_c = 2\exp\left(\int_0^t b\,d\tau\right) = 2\exp(-\Gamma t) \tag{8b}$$

$$\Delta_{a_3}/\Delta_c = 2\exp\left(\int_0^t c\,d\tau\right) = 2 \tag{8c}$$

Under these conditions, $(\Delta_{a_1}\Delta_{a_2}\Delta_{a_3})^{1/3} = 2$. We found that the length scale $(\Delta_{a_1}\Delta_{a_2}\Delta_{a_3})^{1/3}$ is superior to $(\Delta_{a_i}\Delta_{a_j})^{1/2}$. A similar result was found in a study using several anisotropic filters and an isotropic turbulent flowfield. The correlation coefficients obtained using the anisotropic filter for the strained flowfield were slightly improved over those for an isotropic filter. In an isotropic flowfield, on the other hand, anisotropic filters resulted in reduced correlations. While $(\Delta_{a_1}\Delta_{a_2}\Delta_{a_3})^{1/3}$ is the length scale of choice in flowfields with small anisotropy, we must, of course, reserve final judgment on this point until we have studied fields with higher strain. As previously mentioned, this is planned.

IV. Conclusions

The studies we have made of eddy-viscosity-type subgrid-scale models as applied to homogeneous isotropic turbulence and to homogeneous turbulence in the presence of irrotational plane mean strain have led to the following conclusions:

1) The earlier analysis of Ref. 1 was repeated with only small differences in the results. The major conclusion of Ref. 1 is verified: all eddy viscosity models tested perform about the same and demonstrate a modest level of correlation with the exact results. The correlations are, however, less than one would like.

2) The choice of filter type has only a minor influence on the accuracy of an eddy-viscosity subgrid-scale model and is, therefore, a matter of the user's preference.

3) There appears to be an optimum value for filter width. For the flows studied, this width is two to four times the spacing of the grid on which the large-eddy simulation is to be conducted. Outside this range, the accuracy of the model deteriorates badly or the simulation contains too small a proportion of the flow's energy to be meaningful. This also verifies conclusions reached earlier by others.

4) The choice of differencing method used in the model calculations has essentially no effect on the accuracy of the models. The model parameters, on the other hand, are influenced in an important way by the differencing method used. This conclusion is at variance with what others have found.

5) The subgrid-scale Reynolds number $R_{sgs} = \bar{S}\Delta_a^2/\nu$ seems to characterize the subgrid-scale turbulence in the flows

considered. Also, the subgrid-scale models investigated are more accurate at high values of subgrid-scale Reynolds number. For lack of a more accurate alternative, however, they are used in the low Reynolds number range near walls. A relation has been found that represents the variation with subgrid-scale Reynolds number of the scalar-level parameter of the Smagorinsky model. We hope to apply it to channel flow in the near future.

6) The effects of deriving model correlation coefficients and parameters from different realizations of a turbulent flow are negligible.

7) The modified form of the Smagorinsky model suggested in Ref. 13 involving the use of an eddy viscosity averaged over a large volume does not result in significantly improved accuracy, and the effect on the model parameter is small.

8) Higher-order statistical quantities (such as velocity-derivative skewness or flatness) for the resolvable-scale field in a large-eddy simulation cannot be reliably extrapolated to zero filter width to obtain the unfiltered values.

9) For the modest strain rates and strain ratios investigated in this study, no appreciable effects of mean strain on the subgrid-scale models are apparent.

10) In cases where it is desirable to use an anisotropic filter, the appropriate length scale appears to be $(\Delta_{a1}\Delta_{a2}\Delta_{a3})^{1/3}$. This conclusion is based on flows with small anisotropy and must be re-examined in flows with large strain.

Appendix: Definition of the Filter Functions Used Herein

Two filter functions are used in this work. The first is the "box" or "top hat" filter

$$G(x-x') = \begin{cases} \left(\frac{1}{\Delta_a}\right)^3 & |x_i - x_i'| < \Delta_a/2 \quad i=1,2,3, \\ 0 & \text{otherwise} \end{cases} \tag{A1}$$

The other is the Gaussian filter

$$G(x-x') = \prod_{i=1}^{3} \left(\sqrt{\gamma/\pi}\frac{1}{\Delta_{a_i}}\right) \exp\left[-\gamma (x_i - x_i')^2/\Delta_{a_i}^2\right] \tag{A2}$$

where $\gamma = 6$, and the generalized (anisotropic) form is shown.

Fourier transform methods were used to evaluate the convolution integrals necessary to calculate filtered quantities. In these procedures, the discrete transform of the box filter as calculated by a system-provided FFT was used, whereas the continuous transform of the Gaussian filter was used. These choices were made for convenience and do not exert any influence on the results obtained.

Acknowledgment

This work was sponsored by the Office of Naval Research with significant assistance and computer time furnished by the NASA Ames Research Center. In particular we appreciate Robert Rogallo of NASA Ames Research Center for his cooperation in producing the inputs we used and for many useful suggestions.

References

[1] Clark, R. A., Ferziger, J. H., and Reynolds, W. C., "Evaluation of Subgrid-Scale Turbulence Models Using a Fully Simulated Turbulent Flow," Rept. TF-9, Dept. of Mech. Eng., Stanford University, Stanford, Calif., March 1977, to be published in *Journal of Fluid Mechanics*.

[2] Ferziger, J. H. and McMillan, O. J., "Testing of Turbulence Models by Exact Numerical Solution of the Navier-Stokes Equations," NEAR TR 155, Nov. 1977.

[3] McMillan, O. J. and Ferziger, J. H., "Direct Testing of Subgrid-Scale Models," NEAR TR 174, Nov. 1978.

[4] Rogallo, R. S., "An ILLIAC Program for the Numerical Simulation of Homogeneous Incompressible Turbulence," NASA TM-73,203, Nov. 1977.

[5] Ferziger, J. H., "Large Eddy Numerical Simulation of Turbulent Flows," *AIAA Journal*, Vol. 15, Sept. 1977, pp. 1261-1267.

[6] Comte-Bellot, G. and Corrsin, S., "Simple Eulerian Time Correlation of Field- and Narrow-Band Velocity Signals in Grid-Generated Isotropic Turbulence," *Journal of Fluid Mechanics*, Vol. 48, Pt. 2, 1971, pp. 273-337.

[7] Ferziger, J. H., Mehta, U. B., and Reynolds, W. C., "Large Eddy Simulation of Homogeneous Isotropic Turbulence," *Proceedings, Symposium on Turbulent Shear Flows*, The Pennsylvania State University, University Park, Pa., April 1977.

[8] Mansour, N. N., Moin, P., Reynolds, W. C., and Ferziger, J. H., "Improved Methods for Large-Eddy Simulations of Turbulence," *Proceedings, Symposium on Turbulent Shear Flows,* The Pennsylvania State University, University Park, Pa., April 1977.

[9] Shaanan, S., Ferziger, J. H., and Reynolds, W. C., "Numerical Simulation of Turbulence in the Presence of Shear," Rept. TF-6, Dept. of Mech. Eng., Stanford University, Stanford, Calif., Aug. 1975.

[10] Kwak, D., Reynolds, W. C., and Ferziger, J. H., "Three-Dimensional Time Dependent Computation of Turbulent Flows," Rept. TF-5, Dept. of Mech. Eng., Stanford University, Stanford, Calif., May 1975.

[11] Deardorff, J. W., "A Numerical Study of Three-Dimensional Turbulent Channel Flow at Large Reynolds Numbers," *Journal of Fluid Mechanics*, Vol. 41, Pt. 2, 1970, pp. 453-480.

[12] Lilly, D. K., "On the Application of the Eddy Viscosity Concept in the Inertial Sub-Range of Turbulence," NCAR Manuscript No. 123, 1966.

[13] Love, M. D. and Leslie, D. C., "Studies of Sub-Grid Modeling with Classical Closures and Burgers' Equation," *Proceedings, Symposium on Turbulent Shear Flows*, The Pennsylvania State University, University Park, Pa., April 1977.